

Compliance Analysis of A Horizontal Arrangement Parallel Mechanism Considering Gravitational Effect

Peng Xu^{1,2}, Chi Fai Cheung¹, and Bing Li²

¹The Hong Kong Polytechnic University/Department of Industrial and Systems Engineering, Hong Kong, China

²Harbin Institute of Technology/Shenzhen Graduate School, Shenzhen, China

Email: benny.cheung@polyu.edu.hk, libing.sgs@hit.edu.cn

Abstract—A novel polishing machine with serial-parallel mechanism is presented. Since the machine make use of horizontal layout, the gravity of the moving part causes deformation of the end-effector and affects the machining accuracy. As a result, it is essential to analyze the deformation due to gravitational effect. Firstly, the structure and working principle of the serial-parallel polishing machine is introduced. Secondly, the compliance model of the parallel mechanism is formulated based upon the virtual work principle and the deformation superposition principle. The compliance model is established by taking both the deformations of leg system and drive system into account. Hence, the gravity of all moving components and the corresponding deformations are calculated. The results show that gravity has a greater effect on the positional accuracy of the machine. This investigation will provide informative guidelines for optimal stiffness design and gravity compensation of the polishing machine.

Index Terms—compliance analysis; parallel mechanism; gravitational effect; polishing machine

I. INTRODUCTION

As one of the most important steps to machine ultra-precision surface, polishing is used to remove surface cusp and subsurface damage, and then to correct the form. Most of the polishing machines used for fabricating freeform surface are based on the conventional serial mechanisms [1], [2]. Since the cumulative errors of the serial mechanism are difficult to reduce, desired machining results are unable to reach even with high investment. This is a serious impediment to the rapid development of the ultra-precision machining industry. As a result, a novel polishing equipment should be sought to meet the requirements of automated polishing and to improve the machining accuracy.

In recent years, a class of five-axis serial-parallel hybrid configuration equipment represented by Tricept [3], Exechon [4] and VERNE [5] has drawn a widespread attention to the academia and industry. They usually have some favorable characteristics, such as high rigidity, low mobile masses and greater load-to-weight ratio. The

machining equipment built with parallel mechanism as the main structure has been recognized as an advanced solution to machine high-quality products. According to the motion requirements of polishing freeform surface, this paper presents a novel polishing equipment with serial-parallel mechanism and precession polishing process [6].

Stiffness/compliance design is one of the most important link to design a parallel or a serial-parallel configuration equipment. In recent years, many researchers have conducted in-depth study about the stiffness performance of parallel or serial-parallel mechanism. Xu and Li [7] established a stiffness model of a 3PUU parallel mechanism by considering the effect of actuations and constraints based on the screw theory. Tsai and Joshi [8] analyzed the stiffness of a 3RUU parallel mechanism by merely taking into account actuation flexibilities. Cheng et al. [9] built the stiffness model of a 3SPS+1PS parallel mechanism and detected the distributions of stiffness performance within the workspace. In general, the stiffness modeling approaches can be sorted into three main categories which include [10]: the finite elements analysis, the matrix structural analysis and the virtual joint modeling method. It is noted that the horizontal layout parallel mechanism is usually influenced by its own gravity as compared with the vertical layout. The existing studies about the stiffness of parallel mechanism usually ignore the gravitational effect [11] or simplify the gravitational force into a concentrated external force [12]. However, these treatments are insufficient in the case when the change of the center of gravity are not negligible, thus remaining an open issue to be investigated.

This study presents a compliance model of a parallel mechanism in the polishing machine and shows the gravity influence on the accuracy of the end-effector. A novel polishing machine with serial-parallel mechanism is presented. This follows with the kinematics model, while the stiffness model is established together with the study of gravitational effects.

II. STRUCTURE OF THE POLISHING MACHINE

The proposed polishing machine is shown in Fig. 1, which consists of a 2-DOF serial mechanism and a 3-

DOF parallel mechanism. The moving platform of the parallel mechanism is connected to the base by three identical serial chains. Each of the chain contains a prismatic joint and four spherical joints. A fixture that holds the workpiece is mounted on the moving platform. The serial module consists of a rotating/tilting table and a polishing tool. The table is used to rotate the polishing tool about two orthogonal axes. The rotating axis is vertical and tilting axis is horizontal to the base. The curvature center of tool-head is mounted coincides with the virtual pivot intersected by the two axes. The machine uses a horizontal layout which is in favor of polishing slurry flowing into the contact area under the action of gravity.

The polishing machine can provide the motions include: (a) X, Y, Z: positioning of the workpiece to required location; (b) A, B: orientation of the polishing head to follow the local normal direction of the surface and impose the precession angle; (c) H axis: rotation of the polishing head to create the tool influence function; (d) C axis: rotation of the fixture to impose rotational symmetry if required and this is a redundant DOF. This design provides the capability to polish circular and non-circular surface, flats, aspherics, off-axis aspherics and freeform surface. Furthermore, any tool-paths can be implemented.

Since the three rotation axes of the serial manipulator intersect at a virtual pivot, rotations in A and B preserves the same polishing contact area between the polishing tool and the workpiece, causing no XYZ translations. As a result, the motions are decoupled. The positions are all controlled by the parallel module and the orientations are all determined by the serial module. This provides the benefit for the development of control algorithm.

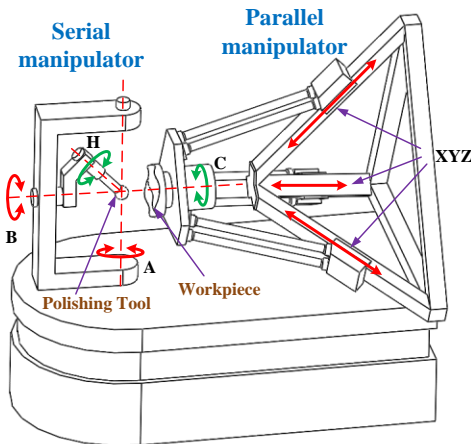


Figure 1. Schematic diagram of the proposed polishing machine.

III. INVERSE POSITION AND JACOBIAN ANALYSIS

The schematic diagram of the parallel mechanism is shown in Fig. 2. The point B_i denotes the actuated prismatic joint. The center of the spherical joint (C_{ij}) that connects the legs with the slider in each of the three chains is denoted as C_i , and the center of the spherical joint (D_{ij}) connected to the moving platform is denoted as D_i . A global reference system O - XYZ is located at the

center of the regular triangle $A_1A_2A_3$ with the Z -axis normal to the base and the X -axis directed along OA_1 . Another local reference system P - uvw is located at the center of the regular triangle $D_1D_2D_3$. The w -axis is perpendicular to the output platform and u -axis directed along PD_1 . E is the reference point of the workpiece on the moving platform.

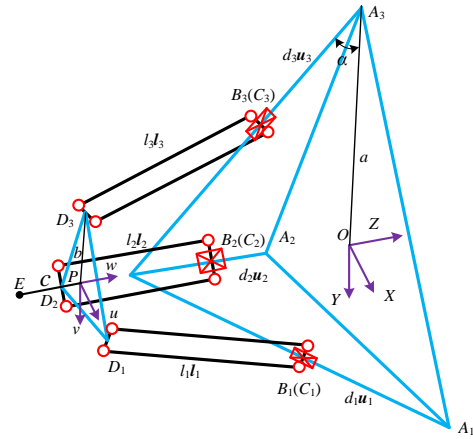


Figure 2. Schematic diagram of the parallel mechanism.

According to the motion characteristics of the parallel mechanism, the three axes of P - uvw are parallel to the corresponding axes of O - XYZ . The related geometric parameters are $OA_i = a$, $PD_i = b$, $PE=c$, $C_iD_i = l$ and $\angle OA_iN = \alpha$.

A vector loop can be written as:

$$\mathbf{P} + \mathbf{b}_i = \mathbf{a}_i + d_i \mathbf{u}_i + l_i \mathbf{l}_i \quad (1)$$

where \mathbf{P} is the position vector of the reference point on the moving platform, d_i and \mathbf{u}_i are the displacement of the i th prismatic joint with respect to A_i and its unit vector, \mathbf{l}_i is the unit vector of i th leg, \mathbf{a}_i and \mathbf{b}_i are the position vectors of A_i and B_i measured in O - XYZ and P - uvw .

When the geometric parameters and \mathbf{P} are given, the results of inverse position analysis d_i can be solved from (1). Equation (1) can also be differentiated with respect to time to obtain the velocity equations, which leads to:

$$\dot{\mathbf{P}} = \dot{d}_i \mathbf{u}_i + \omega_i \times \mathbf{l}_i \quad (2)$$

where ω_i is the angular velocity of chain i .

Multiplying both sides of (2) by \mathbf{l}_i and assembling in matrix form:

$$\dot{\mathbf{d}} = \mathbf{J}_d \dot{\mathbf{P}} \quad (3)$$

where

$$\mathbf{J}_d = \begin{bmatrix} \mathbf{l}_1 & \mathbf{l}_2 & \mathbf{l}_3 \\ \mathbf{l}_1^T \mathbf{u}_1 & \mathbf{l}_2^T \mathbf{u}_2 & \mathbf{l}_3^T \mathbf{u}_3 \end{bmatrix}^T \quad (4)$$

is the Jacobian matrix of the parallel mechanism.

IV. COMPLIANCE MODEL

During the compliance modeling process, the moving platform and base are regarded as a rigid body and the constraints of each joint are ideal constraints. The

schematic diagram of a chain is shown in Fig. 3. The compliance matrix of the leg system and drive system are calculated separately. It is assume that all deformations are small, the compliance matrix of the parallel mechanism can be derived directly according to linear superposition principle:

$$\begin{bmatrix} \Delta \mathbf{X}_E \\ \Delta \boldsymbol{\theta}_E \end{bmatrix} = \begin{bmatrix} \Delta \mathbf{X}_{E,l} \\ \Delta \boldsymbol{\theta}_{E,l} \end{bmatrix} + \begin{bmatrix} \Delta \mathbf{X}_{E,d} \\ \Delta \boldsymbol{\theta}_{E,d} \end{bmatrix} = \mathbf{C} \begin{bmatrix} \mathbf{F}_E \\ \mathbf{M}_E \end{bmatrix} \quad (5)$$

where \mathbf{C} is the compliance matrix of parallel mechanism. $[\mathbf{F}_E^T, \mathbf{M}_E^T]^T$ and $[\Delta \mathbf{X}_E^T, \Delta \boldsymbol{\theta}_E^T]^T$ are the generalized force and the corresponding deformations at E . $[\Delta \mathbf{X}_{E,l}^T, \Delta \boldsymbol{\theta}_{E,l}^T]^T$ and $[\Delta \mathbf{X}_{E,d}^T, \Delta \boldsymbol{\theta}_{E,d}^T]^T$ are the deformations at E due to the compliance of leg system and drive system, respectively. $\mathbf{F}=[F_x, F_y, F_z]^T$ and $\mathbf{M}=[M_x, M_y, M_z]^T$. Similarly, $\Delta \mathbf{X}=[\Delta X_x, \Delta X_y, \Delta X_z]^T$ and $\Delta \boldsymbol{\theta}=[\Delta \theta_x, \Delta \theta_y, \Delta \theta_z]^T$.

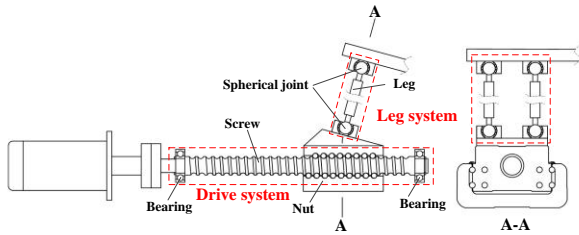


Figure 3. Schematic diagram of chain.

The deformations between P and E have the following relationships:

$$\begin{bmatrix} \Delta \mathbf{X}_{E,l} \\ \Delta \boldsymbol{\theta}_{E,l} \end{bmatrix} = \mathbf{T}_{PE} \begin{bmatrix} \Delta \mathbf{X}_{P,l} \\ \Delta \boldsymbol{\theta}_{P,l} \end{bmatrix} = \begin{bmatrix} \mathbf{E}_3 & -c\hat{\mathbf{w}} \\ \mathbf{0} & \mathbf{E}_3 \end{bmatrix} \begin{bmatrix} \Delta \mathbf{X}_{P,l} \\ \Delta \boldsymbol{\theta}_{P,l} \end{bmatrix} \quad (6)$$

$$\begin{bmatrix} \Delta \mathbf{X}_{E,d} \\ \Delta \boldsymbol{\theta}_{E,d} \end{bmatrix} = \mathbf{T}_{PE} \begin{bmatrix} \Delta \mathbf{X}_{P,d} \\ \mathbf{0} \end{bmatrix} = \begin{bmatrix} \mathbf{E}_3 & -c\hat{\mathbf{w}} \\ \mathbf{0} & \mathbf{E}_3 \end{bmatrix} \begin{bmatrix} \Delta \mathbf{X}_{P,d} \\ \mathbf{0} \end{bmatrix} \quad (7)$$

where $[\Delta \mathbf{X}_{P,l}^T, \Delta \boldsymbol{\theta}_{P,l}^T]^T$ and $[\Delta \mathbf{X}_{P,d}^T, \mathbf{0}^T]^T$ are the deformations at P due to the compliance of leg system and drive system, respectively. The corresponding force at P is $[\mathbf{F}_P^T, \mathbf{M}_P^T]^T$. \mathbf{E}_3 stands for a unit matrix of order 3. \mathbf{w} is the unit vector between the two point and $\hat{\mathbf{w}}$ stands for the antisymmetric matrix of vector \mathbf{w} .

A. Compliance Matrix of Leg System

According to the principle of virtual work, the following equation can be obtained:

$$\begin{bmatrix} \Delta \mathbf{X}_{P,l}^T & \Delta \boldsymbol{\theta}_{P,l}^T \end{bmatrix} \begin{bmatrix} \mathbf{F}_P \\ \mathbf{M}_P \end{bmatrix} = \Delta \mathbf{l}^T \mathbf{f}_l, \quad \Delta \mathbf{l} = \mathbf{C}_l \mathbf{f}_l \quad (8)$$

where \mathbf{f}_l , $\Delta \mathbf{l}$ and \mathbf{C}_l are the force matrix, deformation matrix and compliance matrix of the leg system.

The force at P and the reaction force of leg system have the following relations:

$$\mathbf{J}_l \mathbf{f}_l = \begin{bmatrix} \mathbf{F}_P \\ \mathbf{M}_P \end{bmatrix} \quad (9)$$

where

$$\mathbf{J}_l = [\mathbf{J}_{1l} \quad \mathbf{J}_{2l} \quad \mathbf{J}_{3l}]^T, \quad \mathbf{J}_{il} = \begin{bmatrix} l_i & l_i \\ \mathbf{b}_{i1} \times l_i & \mathbf{b}_{i2} \times l_i \end{bmatrix} \quad (10)$$

in which \mathbf{b}_{i1} and \mathbf{b}_{i2} denote the vectors of PD_{i1} and PD_{i2} .

According to Eq. (6), Eq. (8) and Eq. (9), the deformation and the compliance matrix due to the leg system are:

$$\begin{bmatrix} \Delta \mathbf{X}_E \\ \Delta \boldsymbol{\theta}_E \end{bmatrix} = \mathbf{C}_1 \begin{bmatrix} \mathbf{F}_E \\ \mathbf{M}_E \end{bmatrix} \quad (11)$$

$$\mathbf{C}_1 = \mathbf{T}_{P,E} \mathbf{J}_l^{-T} \mathbf{C}_l \mathbf{J}_l^{-1} \mathbf{T}_{P,E}^T \quad (12)$$

where \mathbf{C}_l is the compliance matrix of leg system.

\mathbf{C}_l can be derived from the corresponding stiffness matrix \mathbf{K}_l . As shown in Fig. 3, \mathbf{K}_l can be expressed as:

$$\mathbf{K}_l = \text{diag} [k_{ij}^l] \quad (13)$$

where the diagonal element k_{ij}^l represents the axial tension and compression stiffness coefficient of leg system j in chain i . Each leg system can be regarded as a spring system connected serially by two spherical joints and one leg.

B. Compliance Matrix of Drive System

The axial deformation of the drive system only causes the moving platform to experience translational deformation $\Delta \mathbf{X}_d$. According to the principle of virtual work, the following equation can be obtained:

$$\Delta \mathbf{X}_{P,d}^T \mathbf{F}_P = \Delta \mathbf{d}^T \mathbf{f}_d, \quad \Delta \mathbf{d} = \mathbf{C}_d \mathbf{f}_d \quad (14)$$

where \mathbf{f}_d , $\Delta \mathbf{d}$ and \mathbf{C}_d are the force matrix, deformation matrix and compliance matrix of the drive system.

The deformations of moving platform and drive system have the following relations:

$$\Delta \mathbf{d} = \mathbf{J}_d \Delta \mathbf{X}_{P,d} \quad (15)$$

According to Eqs. (7), Eq. (14) and Eq. (15), the deformation and the compliance matrix due to the drive system are:

$$\begin{bmatrix} \Delta \mathbf{X}_E \\ \Delta \boldsymbol{\theta}_E \end{bmatrix} = \mathbf{C}_2 \begin{bmatrix} \mathbf{F}_E \\ \mathbf{M}_E \end{bmatrix} \quad (16)$$

$$\mathbf{C}_2 = \mathbf{T}_{P,E} \mathbf{T} \mathbf{J}_d^{-1} \mathbf{C}_d \mathbf{J}_d^{-T} \mathbf{T}^T \mathbf{T}_{P,E}^T \quad (17)$$

where \mathbf{C}_d is the compliance matrix of drive system and $\mathbf{T}_{6 \times 3} = [\mathbf{E}_3, \mathbf{0}]^T$ is the transformation matrix.

\mathbf{C}_d can be derived from the corresponding stiffness matrix \mathbf{K}_d . As shown in Fig.3, \mathbf{K}_d can be expressed as:

$$\mathbf{K}_d = \text{diag} [k_i^d] \quad (18)$$

where the diagonal element k_i^d represents the axial tension and compression stiffness coefficient of drive system in chain i . Each drive system can be regarded as a

spring system connected serially by bearing, screw and nut.

V. DEFORMATIONS DUE TO THE GRAVITATIONAL EFFECT

In summary, the compliance matrix of the parallel mechanism can be derived by substituting (11) and (16) into (5):

$$C = C_1 + C_2 \quad (19)$$

According to the compliance model, the deformation of the parallel mechanism $[\Delta X_{g,E}^T, \Delta \Theta_{g,E}^T]^T$ due to the gravity can be expressed as:

$$\begin{bmatrix} \Delta X_{g,E} \\ \Delta \Theta_{g,E} \end{bmatrix} = C \begin{bmatrix} F_{g,E} \\ M_{g,E} \end{bmatrix} \quad (20)$$

where $[F_{g,E}^T, M_{g,E}^T]^T$ is the generalized force vector at E due to the gravity of each moving components and it satisfies:

$$\begin{bmatrix} F_{g,E} \\ M_{g,E} \end{bmatrix} = T_{EC_p}^{-T} F_{g,P} + 2 \sum_{i=1}^3 T_{EP}^{-T} T_{PC_{l,i}}^{-T} F_{g,l} \quad (21)$$

where T_{EC_p} is the transformation matrix between the gravity center of the moving platform C_p (as shown in Fig. 4) and E ; T_{EP} is the transformation matrix between P and E ; $T_{PC_{l,i}}$ is the transformation matrix between the gravity center of leg $C_{l,i}$ and P . $F_{g,P}$ and $F_{g,l}$ represent the six-dimensional gravity vector of moving platform and leg, respectively.

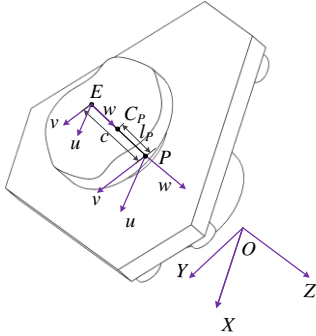


Figure 4. Structured of the moving platform

These matrixes can be expressed as:

$$F_{g,P} = \begin{pmatrix} m_P \mathbf{g} \\ \mathbf{0} \end{pmatrix}, F_{g,l} = \begin{pmatrix} m_l \mathbf{g} \\ \mathbf{0} \end{pmatrix} \quad (22)$$

$$T_{EC_p} = \begin{bmatrix} E_3 & \hat{r}_{EC_p} \\ \mathbf{0} & E_3 \end{bmatrix}, T_{EP} = \begin{bmatrix} E_3 & \hat{r}_{EP} \\ \mathbf{0} & E_3 \end{bmatrix},$$

$$T_{PC_{l,i}} = \begin{bmatrix} E_3 & \hat{r}_{PC_{l,i}} \\ \mathbf{0} & E_3 \end{bmatrix} \quad (23)$$

where

$$\begin{cases} r_{EC_p} = (c - l_p) \mathbf{w} \\ r_{EP} = c \mathbf{w} \\ r_{PC_{l,i}} = \mathbf{b}_i - l_i l_i \end{cases} \quad (24)$$

in which l_p is the distance from C_p to P and l_i is the distance from $C_{l,i}$ to the spherical joint on the moving platform.

Since gravity has the most significant impact on the deformation of the parallel mechanism along the gravity direction, the translational deformation of E in the workspace along Y axis are used to show the influence of gravitational effect. The gravity parameters, structural parameters of the parallel mechanism are listed in Table I and Table II, respectively. The task workspace of P is a cuboid with $h=50$ mm and $s=100$ mm as shown in Fig. 5. The stiffness parameters of leg system k_i^l and drive system k_i^d are 200 N/ μ m and 150 N/ μ m, respectively.

TABLE I. GRAVITY PARAMETERS OF THE PARALLEL MECHANISM

Moving platform		Leg	
m_P /kg	l_P /mm	m /kg	l /mm
20	-17	2	223.6

TABLE II. STRUCTURAL PARAMETERS OF THE PARALLEL MECHANISM

l (mm)	α (deg)	a (mm)	b (mm)	c (mm)	d (mm)
447.2	45°	400	100	60	70

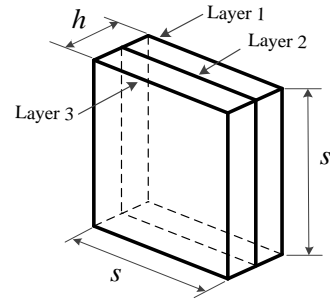
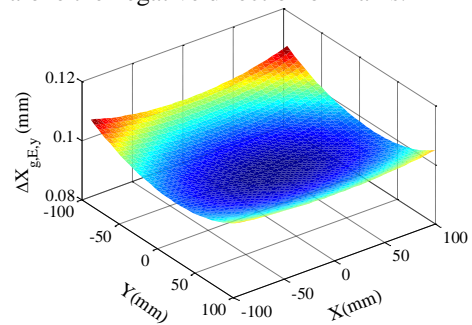


Figure 5. Typical configurations within workspace

Fig. 6 shows the deformation distribution of E in three different lays in the workspace. Clearly, gravity of the moving components has a significant influence on the position accuracy of the parallel mechanism. $\Delta X_{g,E,y}$ has a symmetrical distribution about $X=0$ mm plane. This is consistent with the global reference system and the symmetrical structure of the parallel mechanism. The deformations are increased when the parallel mechanism moves along the negative direction of Z axis.



(a) Layer 1 $Z = -550$ mm

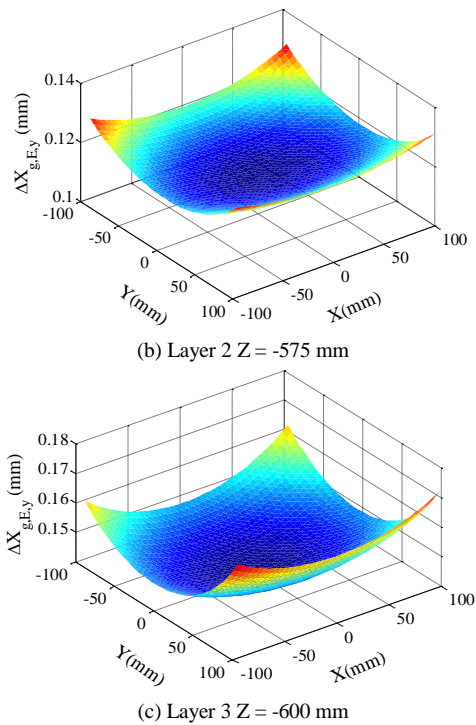


Figure 6. Distribution of Y-direction deformation in the workspace

Fig. 7 shows the deformation distribution of E in layer 2 caused separately by the deformation of leg system and drive system. As shown in Fig. 7, the deformations of the parallel mechanism are mainly influenced by the leg system. In fact, which one has the bigger influence or smaller influence is depended on the structure and stiffness parameter of the each system. In return, these distributions can provide guidance for improving the design.

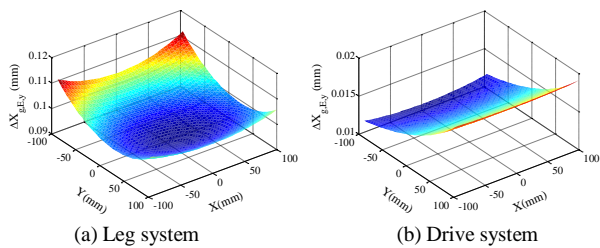


Figure 7. Contribution of the main component to deformation in layer 2 with $Z = -575$ mm

VI. CONCLUSIONS

This paper proposes a new polishing machine with serial and parallel mechanism. By taking gravity into account, the compliance analysis of the parallel mechanism is conducted. The following conclusions are drawn:

- The compliance model of the parallel mechanism is established based on the inverse kinematics and

Jacobian matrix considering the influence of leg system and drive system.

- The gravity of moving components, including the moving platform and leg, has a significant influence on the position accuracy of the parallel mechanism, leading to an issue in need of structural optimization and gravity compensation in further studies.

ACKNOWLEDGMENT

The authors would like to express their sincere thanks to the Innovation and Technology Commission (ITC) of the Government of the Hong Kong Special Administrative Region (HKSAR) for the financial support of the research work under the projects No. GHP/031/13SZ. The work was also supported by Shenzhen Research Funds Grants under the projects No. SGLH20131010144128266, ZDSYS20140508161825065.

REFERENCES

- [1] C. F. Cheung, L. B. Kong, L. T. Ho, and S. To, "Modelling and simulation of structure surface generation using computer controlled ultra-precision polishing," *Precis Eng*, vol. 35, no. 4, pp. 574-590, 2011.
- [2] D. Feng, Y. Sun, and H. Du, "Investigations on the automatic precision polishing of curved surfaces using a five-axis machining centre," *Int. J. Adv Manuf Tech*, vol. 72, no. 9, pp. 1625-1637, 2014.
- [3] F. Caccavale, B. Siciliano, and L. Villani, "The Tricept robot: dynamics and impedance control," *IEEE-ASME T Mech*, vol. 8, no. 2, pp. 263-268, 2003.
- [4] Z. M. Bi and Y. Jin, "Kinematic modeling of exechon parallel kinematic machine," *Robot Com-Int Manuf*, vol. 27, no.1, pp. 186-193, 2011.
- [5] D. Kanaan, P. Wenger, and D. Chablat, "Kinematic analysis of a serial-parallel machine tool: The VERNE machine," *Mech Mach Theory*, vol. 44, no. 2, pp. 487-498, 2009.
- [6] D. Walker, D. Brooks, A. King, R. Freeman, R. Morton, G. McCavana, and S. W. Kim, "The 'Precessions' tooling for polishing and figuring flat, spherical and aspheric surfaces," *Opt Express*, vol. 11, no. 8, pp. 958-964, 2003.
- [7] Q. Xu and Y. Li, "An investigation on mobility and stiffness of a 3-DOF translational parallel manipulator via screw theory," *Robot Com-Int Manuf*, vol. 24, no. 3, pp. 402-414, 2008.
- [8] L. W. Tsai and S. Joshi, "Kinematic analysis of 3-DOF position mechanisms for use in hybrid kinematic machines," *ASME J. Mech Design*, vol. 124, no. 2, pp. 245-253, 2002.
- [9] G. Cheng, J. Yu, P. Xu, and H. Liu, "Stiffness analysis of the 3SPS+1PS bionic parallel test platform for a hip joint simulator," *Robotica*, vol. 31, no. 6, pp. 935-944, 2013.
- [10] A. Klimchik, D. Chablat, and A. Pashkevich, "Stiffness modeling for perfect and non-perfect parallel manipulators under internal and external loadings," *Mech Mach Theory*, vol. 79, pp. 1-28, 2014.
- [11] Y. Li and Q. Xu, "Stiffness analysis for a 3-PUU parallel kinematic machine," *Mech Mach Theory*, vol. 43, no. 2, pp. 186-200, 2008.
- [12] G. Cheng, P. Xu, D. Yang, et al., "Stiffness analysis of a 3CPS parallel manipulator for mirror active adjusting platform in segmented telescope," *Robot Com-Int Manuf*, vol. 29, no. 5, pp. 302-311, 2013.